Global Advanced Research Journal of Engineering, Technology and Innovation (ISSN: 2315-5124) Vol. 2(10) pp. 295-303, October, 2013
Available online http://garj.org/garjeti/index.htm

Full Length Research Paper

Mapping And Analysis Of The Density Of Lineaments Around Kagoro Younger Granite Rocks In North Central Nigeria

Samaila Crah Alkali

Department of Geology University of Maiduguri, P. M. B. 1069, Maiduguri, Nigeria
Corresponding Email: samcrah@gmail.com; Tel: +2348069263114

Accepted 14 October 2013

Mapping and analysis of the density of lineaments around Kagoro Younger Granite complex and environs were conducted by visual and manual inspections from four data sources, which were later combined to form the fifth source. Positively skewed values are characteristic results of statistical analysis of the data. Numerical values of lineament frequencies in the various class intervals range from zero for relatively stable environments to fifty where intensity of emplacement of the rock bodies were relatively high. Major lineament trends were found in conjugate NE - SW and NW - SE orientations. Main structural directions of the rose diagrams are the NE – SW and NW – SE and the structurally directions derived from 2D maps are aligned along NE – SW, NW – SE and ENE – WNW. These trends are consistent with the trends of the Nigerian Basement Complex and the Younger Granite complex. The density and orientation of the fracture lines revealed areas of greater lineament development in the north central occurring over the surface expression of the Kagoro intrusion and other rock units.

Keywords: Density, Frequency, Lineament, Orientation, Rose diagram

INTRODUCTION

Rock movement below the earth surface generates stress that produces deformational effects capable of changing the shapes of the rock by fracturing. Joints and other linear structures can be observed in every rock exposure (Maltman, 1990). These structures are generally oriented along the N – S, NE – SW, NW – SE and sometimes E – W trends (Wright, 1976; Oluyide, 1988; Udoh, 1988, Olasehinde and Awojobi, 2004). Linear features are usually good exploratory targets as they aid migration of fluids and host accumulation of minerals of economic importance.

The Younger Granite complexes of Nigeria in which the Kagoro granite is a part trend in an N – S belt with the ages of the complexes decreasing southwards. Rahaman et al (1984) showed that major local magmatic activities were concentrated along ENE and WSW zones. The age pattern suggests that the parent magma were locally derived from several simultaneous high level magma chambers connected to a common deeper source. Emplacement of these ring complexes was controlled by fracture systems in the basement.

The study area shown in Fig. 1 lies between latitudes

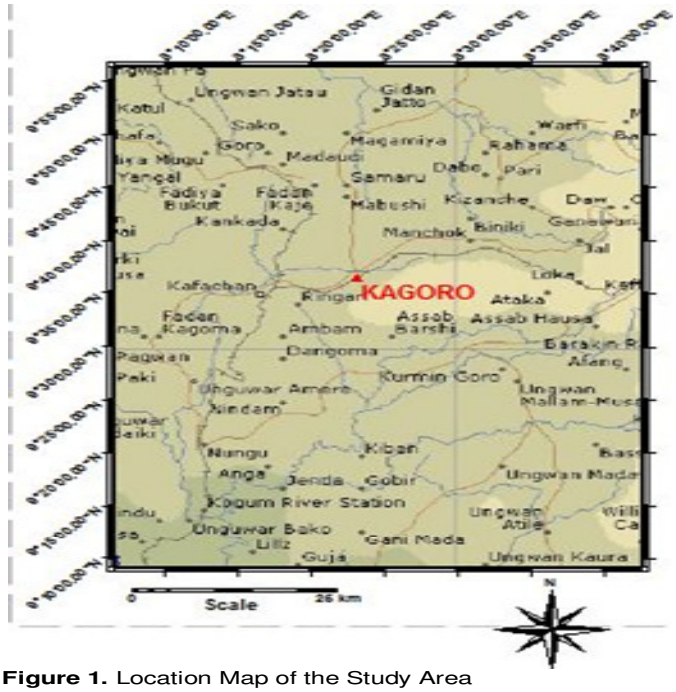

Figure 1. Location Map of the Study Area

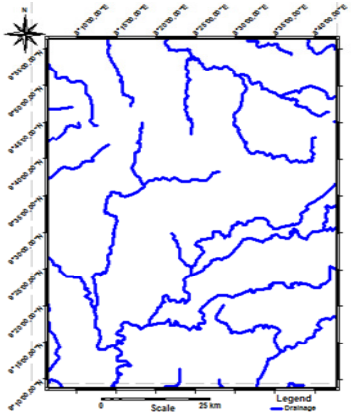

2a Drainage Lineament

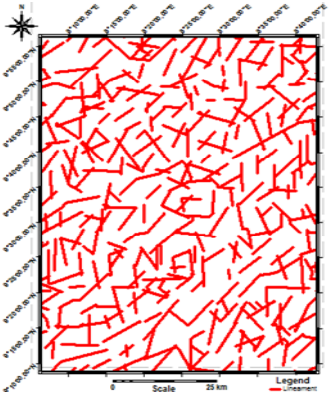

2b Satellite Lineament

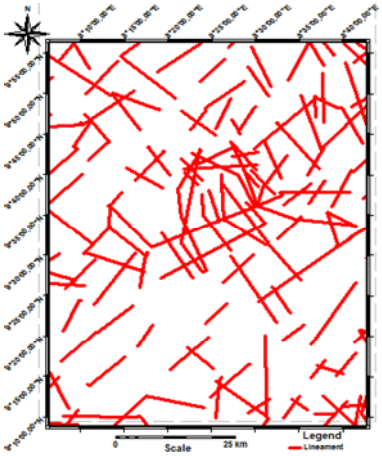

2c Magnetic Lineament

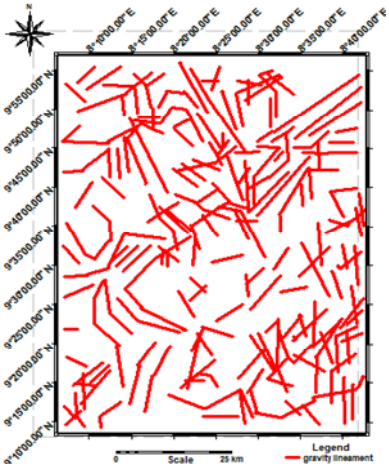

2d of Gravity Lineament

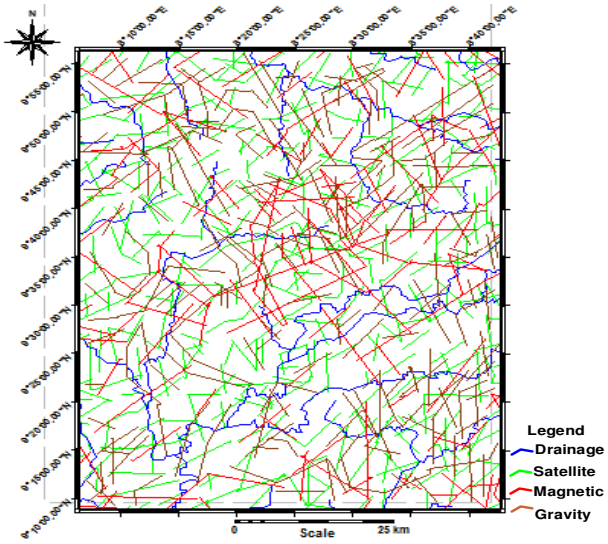

2e Combined Lineaments

Figure 2. Source Data of the Lineaments

Table 1. Coordinate Projection Parameters

Projection	Datum Area	Datum	Ellipsoid Parameters		Ellipsoid	Hemisphere	Zone
UTM	Nigeria	Minna	a	6378249	Clarke, 1880	Northern	32
			1/f	293.465			

(Source, ILWIS, 2005)

Table 2. Statistical Distribution of the Lineaments

Lineament Source	Lineament Length Characteristics (km)					
	Sum	Minimum	Maximum	Mean	Standard Deviation	Skewness
Drainage	1051.69	0.49	27.18	5.84	5.19	1.09
Satellite	1012.10	0.97	20.87	5.62	4.58	0.87
Magnetic	1062.61	0.34	30.33	5.90	5.44	1.04
Gravity	1063.31	0.39	30.03	5.68	5.01	0.71
Merged	1554.60	0.34	28.68	8.64	5.63	0.80

9°08'41.2" – 9°56'22.5" N and between longitudes 8°06'30.0" – 8°42'51.2" E. This translates to approximate area coverage of 5827 km^2. This work is intended at using the results of interpolated lineament density data extracted from drainage, satellite, aeromagnetic, gravity and their overlays to infer their structural trends in relation to the emplacement of the Kagoro Younger Granite complex and other rock units.

Geology of the Younger Granite

The Younger Granite complexes of Nigeria comprise of Precambrian to Lower Paleozoic Basement Complex rocks into which the Younger Granites suites are emplaced (MacLeod et al, 1965). Basement rocks cover about three quarters of the Younger Granite complexes and consist of ancient sediments of granulitic gneiss, dioritic rocks, migmatites, granite-gneiss, older granites and granodiorites (MacLeod et al, 1965; Oyawoye, 1964 and 1972). Cone sheets and ring dykes are widely distributed. The ring dykes dip outwardly both on the inner and outer contacts but some have steep or vertical contacts (MacLeod et al, 1965).

The Younger Granite complexes trend in an N – S belt with the ages of the complexes decreasing southwards. Rahaman et al (1984) pointed out that major local magmatic activities were concentrated along ENE and WSW zones. The age pattern suggests that the parent magma were locally derived from several simultaneous

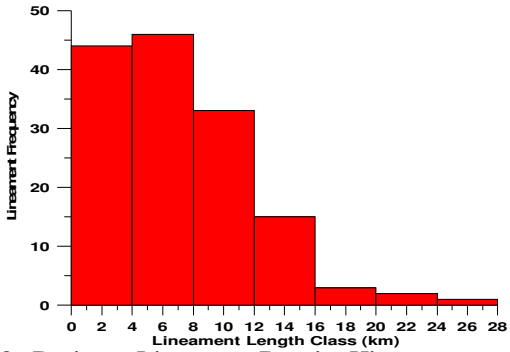

3a Drainage Lineament Density Histogram

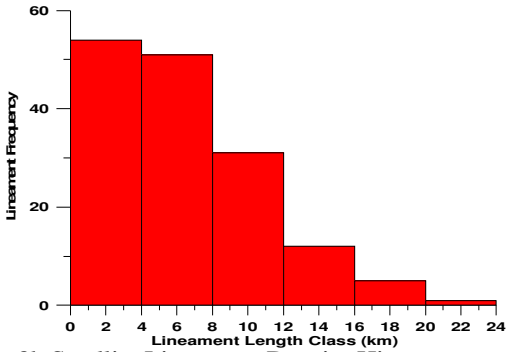

3b Satellite Lineament Density Histogram

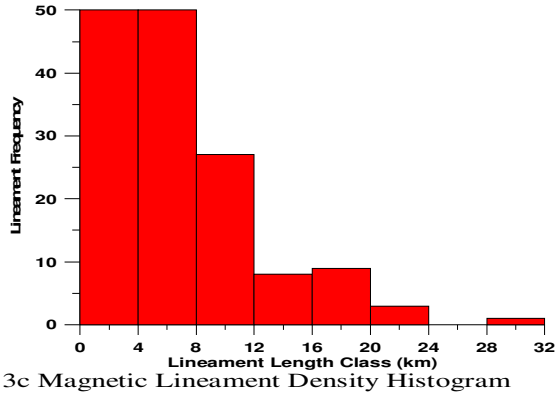

3c Magnetic Lineament Density Histogram

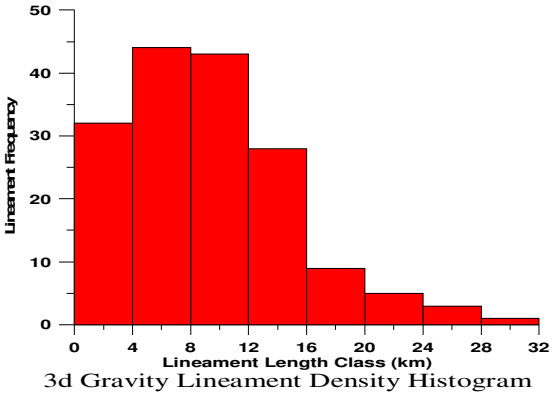

3d Gravity Lineament Density Histogram

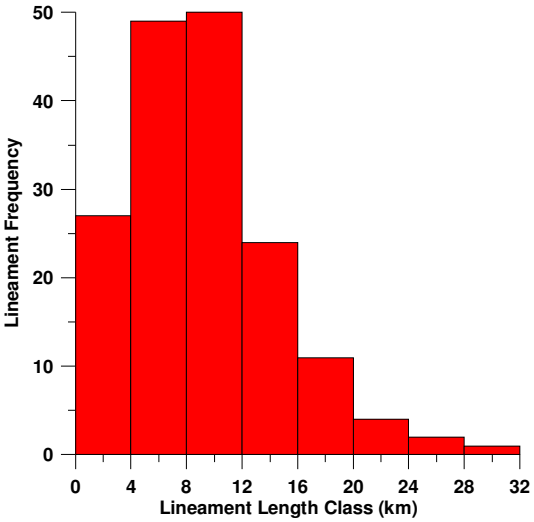

3e Combined Lineament Density Histogram

Figure 3. Lineament Density Histograms

high level magma chambers connected to a common deeper source. Emplacement of these ring complexes was controlled by fracture systems in the basement

The main phase of acid magmatism in Nigerian Younger Granite complexes commenced during Triassic times and continued to migrate in a southerly direction until the close of the Jurassic (Bowden et al, 1971). The cessation of magmatism was synchronous with the initiation of the South Atlantic.

Turner (1989) proposed three stages of development of the Nigerian ring complexes. These are:

i The early stage of a large rhyolite volcano which prior to the end of its stage, large amount of magma accumulated in the synvolcanic reservoir about five kilometers beneath the surface.

ii Caldera and ring dyke stage when the centre of the volcanic structure within a ring fault collapsed, magma arose along the fault and crystallized as granite porphyry which was extruded into the caldera rocks

iii Intrusive stages were the waning phase of igneous activity when smaller granite intrusions were emplaced at increasing deep levels. The magma evolved

Table 3. Lineament Orientation Trends

Data Type	Number of Trends	Orientation Description			
		1°	**2°**	**3°**	**4°**
Drainage	4	N 5° E	N 55° E	(a) N 55° W (b) N 25° W	-
Satellite	4	N 5° E	N 5° W	N 75° W	N 35° W
Magnetic	4	N 5° E	N 5° W	N 75° W	N 55° W
Gravity	5	N 5° E	N 25° E	(a) N 25° W (b) N 35° W (c) N 5° W	-
Combined	5	N 5° E	(a) N 45° E (b) N 35° W	(a) N 85° E (b) N 65° W	-

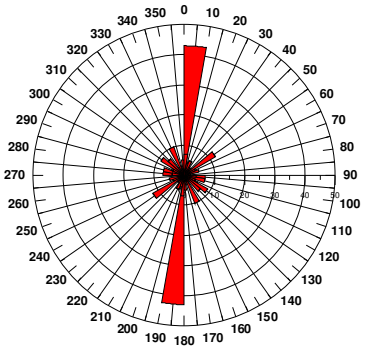

4a Drainage Lineament Density Rose Diagram

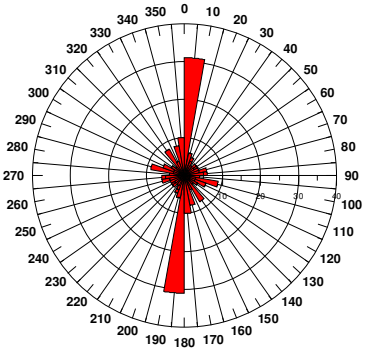

4b Satellite Lineament Density Rose Diagram

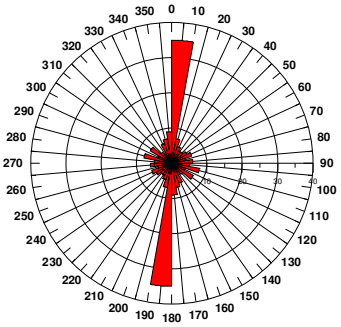

4c Magnetic Lineament Density Rose Diagram

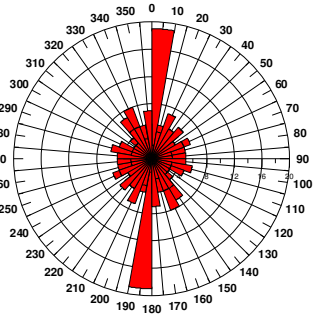

4d Gravity Lineament Density Rose Diagram

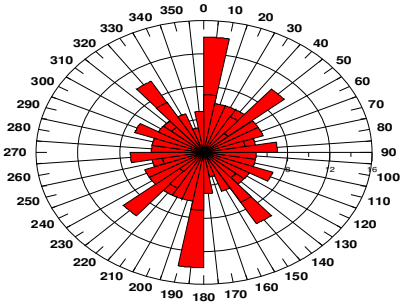

4e Combined Lineament Density Rose Diagram

Figure 4. Lineament Density Rose Diagrams

and crystallized at lower temperatures and as lower assemblages. They rocks are composed of biotite granite.

The Younger Granites have a clear topographical definition and there is usually a close coincidence between the geological and topographical boundaries at the margins of the granites. They form continuous ranges and plateaus, which rise between 91 and 305 m above the surrounding level plains (MacLeod et al, 1965). The Younger Granites are underlain by older granites, migmatites and meta-sediments of the basement complex.

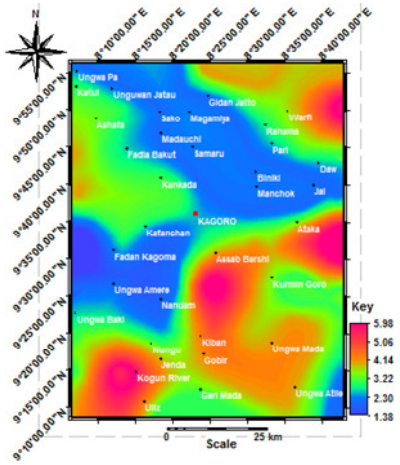

5a Drainage Lineament Density Map

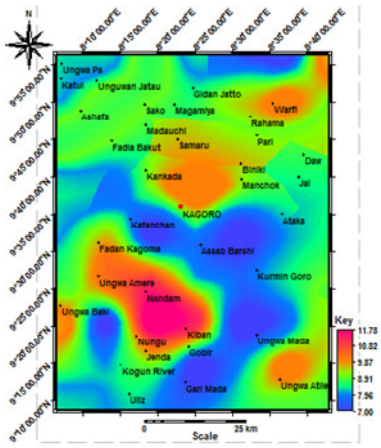

5b Satellite Lineament Density Map

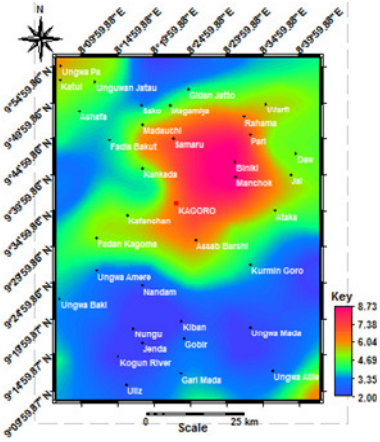

5c Magnetic Lineament Density Map

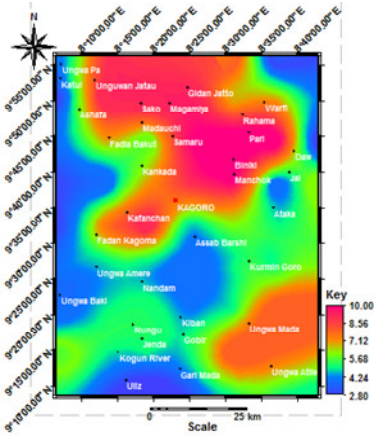

5d Gravity Lineament Density Map

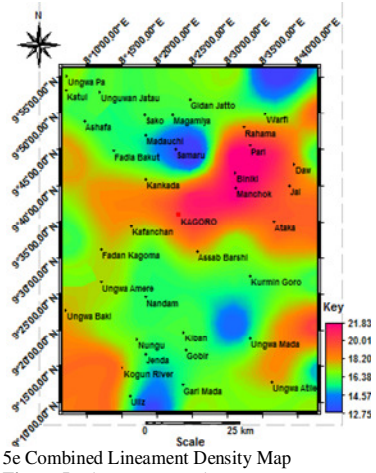

5e Combined Lineament Density Map

Figure 5. Lineament Density Maps

MAPPING AND ANALYSIS METHODS

Identification and analysis of lineaments from drainage, satellite, magnetic, gravity and combination of these sources were conducted by visual and manual inspection of each of the data and imagery on the same scale. Lineaments in Fig. 2 were identified and digitized on screen using the tools in Integrated Land and Watershed Information System3.3 (2005) (ILWIS 3.3)) software. The same software was used to georeferenced all the maps. Individual lineaments were analyzed for direction trends in the ILWIS 3.3 (2005) submenu. Rose diagrams were

created from the lineaments maps and presented as directional trends on 10° orientation class intervals in Grapher5 (2004) environment. Individual lineament lengths were statistically analyzed and plotted on frequency distributions of lineaments length per lineament length class also in the same Grapher5 (2004) environment.

The four sources of the lineaments were superimposed into a single map. Lineament density was calculated for each section of cell of the source data using the total lineaments lengths contained within each unit section. Nodes were determined at the central points of each of the sections in ILWIS 3.3 (2005) for extraction of geographic coordinates and data file management of corresponding lineament density values.

The resulting X, Y, Z data file was imported into Surfer9 (2009) software for contouring using kriging interpolation algorithm. The interpolated density contours were exported from Surfer9 (2009) into ILWIS 3.3 (2005) for spatial projection.

Coordinate Projection

Prominent features positioning on all maps were georeferenced using the Universal Transverse Mercator (UTM) system in ILWIS (2005) environment. UTM system divides the earth into sixty discrete zones, each representing a vertical slice of the globe spanning six degrees of longitude. A Transverse Mercator projection is applied to each zone with the central meridian of the projection at the centre of the given zone and the central latitude of the projection at the equator.

The scale factor at the central meridian by definition is 0.9996, and distance measurements on the maps used this scale factor. The Clarke 1880 given in ILWIS (2005) ellipsoid was applied. Coordinate projection parameters for this study are given in Table 1.

DATA ANALYSIS

Descriptive statistical analysis results gave the cumulative distance of both the streams and the rivers derived from the drainage lines in the area at 1051.69 km and its average at 5.84 lineaments per kilometre (Table 2). The total length of the lineaments from the satellite image is 1012.10 km and its average is 5.62 lineaments per kilometre. Magnetic lineaments' data produced cumulative length of 1062.61 km and average of 5.90 lineaments per kilometre. The gravity data cumulative length of the lineaments is 1063.31 km. This yielded data mean of 8.68 lineaments per kilometre. Combined lineaments have total length of 1554.60 km and average of 8.64 lineaments per kilometre.

Lineament Density Histograms

The most common method of graphical data presentation is the histogram, which is a plot of the proportional frequency of observed values lying within given numerical values. The ordinate of the plot is obtained by dividing the number of values within the particular interval by the total number of values. For the purpose of this work, the frequency of the lineaments was plotted against the lineament length class. The lineament density lengths of the histograms in Fig. 3 were grouped into class intervals of four.

The histogram of drainage lineament density in Fig. 3a is positively skewed with the highest lineament frequency of 47 occurring within class interval of 4 – 8 and the lowest lineament frequency of one occurring within the class interval of 24 – 28. Satellite histogram of the lineament density shown in Fig. 3b is also positively skewed. The class interval within 0 – 4 has lineament frequency of 47, while the range within the 20 – 24 class has lineament frequency value of 2.

In Fig. 3c magnetic lineament density histogram produces two major lineament frequencies of magnitude 50 each within class intervals of 0 – 4 and 4 – 8. A lineament frequency of one only was recorded within the class range of 28 – 32 while the interval of 24 – 28 did not record any lineament length frequency. Lineament length density within the class interval of 4 – 8 of the gravity histogram produces lineament frequency of 44 while the class interval within the 28 – 32 range contains 2 lineaments (Fig. 3d).

Combined lineament density histogram in Fig. 3e produces numerical lineament frequency value of 50 within the class interval of 8 – 12. The lineament density within the class of 28 – 32 produces lineament frequency of 2.

Lineament Density Orientations And Rose Diagrams

Directional data extracted during analysis of the fractures are summarized on Table 3 and presented in rose diagrams in Figs 4.

For the rose diagrams the trend and/or strike data are organized into bin sizes (class intervals) of 10°, where each bin represents the number of values that fall within the specific angular region. A family of concentric circles provides scaled control for the number of fracture-orientation values that occupy each bin size.

Drainage lineament density rose diagram in Fig. 4a produces a primary 1° trend of N 5° E along with a tertiary 3° conjugate trend of N 55° W; the same primary 1° trend of N 5° E trend along with a tertiary 3° trend of N 25° W and a tertiary 3° trend of N 55° W along with a conjugate tertiary 3° trend of N 25° W. Within the satellite imagery

lineament density rose diagram (Fig. 4b), only one secondary 2^o trend of N 5^o W along with a conjugate quaternary 4^o trend of N 55^o W is prominent.

Fig. 4c of the magnetic lineaments density rose diagram displays a primary 1^o trend of N 5^o E along with a conjugate 4^o trend of N 55^o W. Rose diagram of Fig. 4d produced from gravity lineament density recorded a primary 1^o trend of N 5^o E along with a conjugate tertiary 3^o trend of N 25^o W, a secondary 2^o trend of N 25^o E along with a conjugate tertiary 3^o trend of N 35^o W and a secondary 2^o trend of N 25^o E along with another tertiary 3^o conjugate trend of N 5^o E. Combination of the lineaments' azimuth data given in Fig. 4e resulted in identifying a secondary 2^o trend of N 35^o W along with a tertiary 3^o conjugate trend of N 65^o W.

LINEAMENT DENSITY MAPS

Lineament density maps display the distributions of the lineaments in two-dimensional maps. The area was divided into equal area grids. The number of lineaments in each grid were counted and recorded. A lineament that extended into another domain boundary was counted within the grid area extended into. The numbers were assigned to the centre of each grid area and then contoured at appropriate intervals. Interpolated contour pseudo representations of the lineament density maps for the five sources of the lineaments data are shown on Figs. 5a – 5e.

The map of the drainage lineament density in Fig. 5a produces low density linear structures (1.30 – 2.40) along a NW – SE direction at the northeastern, the north central and the western parts. Structural features of low density values are observed also at the extreme edge of the southeast. Intermediate values lineament density structures from 2.40 - 4.00 sandwiches both the low and high lineament density structures within the entire map. High values lineament density features are observed around the southern part; predominantly along the southeast. Also a high value lineament density structural area is at the extreme edge of the northeast.

Majority of low values structural lines of the satellite lineament density map (Fig. 5b) occur at the southern half. These structures enclose intermediate and high values lineament density structures at the southwest. Lineaments density structures of low values are also encountered at the extreme north and northwest parts. Their values lie within domains of 7.00 – 7.60. Lineament structural density of intermediate values around 7.60 – 9.00 occupy more than half of the area and are sandwiching those of high structural density values throughout the map. High lineament density values within 7.60 - 11.75 interval trend along the NE – SW at the northern part and strike in the NW – SE at the western part. In place they are separated by low and intermediate values lineament density structures at the southern half. Magnetic lineament density structural values lower than 4.00 (Fig. 5c) are align in a narrow belt along the NE – SW direction around the northwest and trend in the ENE – WNW direction in the south. Intermediate lineament density structural values (3.40 – 6.00) envelope high values lineament density structural units. The same intermediate values structures occupy the edges of the extreme NW and SE. Densely populated lineament structures occupy the central, north central and a small portion of the southeastern edge. Density values of these features range from around 6.00 – 8.70.

Fig. 5d is a 2D map produced from gravity lineament density data. The low values lineament density structures occur in patches mainly at the southern half of the area. Their structural values range from 2.8 – 4.3. These structures align in the NE – SW direction at the southern part. NE – SW trending lineament density structures of intermediate values (4.30 – 6.80) enclose low values lineament density structures in the southern part. The intermediate values lineament density structures cover up to thirty five percent of the area. Lineament density structural values of 6.80 - 10.00 form lineament density of high structural values. These linear features cover more than forty percent of the area and are found mainly at the northern and southeastern parts.

Low structural values approximately 12.90 – 15.00 of the combined lineament density in Fig. 5e lie within four isolated domains which consists of two pockets at the south and two pockets at the north. These lineament density structures trend along the NE – SW direction. Lineament density structures of intermediate values in the range of 15.00 – 17.00 occupy about sixty percent of the area. They occur at the southern half and the northern parts. High values lineament density structures are observed in the north central, southwest and southeast. Their values range from about 17.00 – 21.80.

CONCLUSION

Four data sources of lineaments were identified and mapped. These were overlaid to form the fifth source of lineament data. Statistical analysis on the data produced positively skewed indices. Lineaments frequency values within the various class intervals range from zero in the environments where magmatic activity was relatively stable to fifty in the environments of major activity. Structural trends along the NE – SW, NW – SE and the ENE – WNW responded to both stress difference and orientation of the principal stresses. The NE - SW set is interpreted as belonging to fractures generated by tectonics activities (Alkali and Yusuf, 2010). The surface expression of the Kagoro intrusion is revealed by high

lineament density.

REFERENCES

Alkali SC, Yusuf SN (2010). Gravity Study over Jos – Bukuru Younger Granite Complex, North Central Nigeria. Scholars Research Library, Archives of Physics Research, 1(4): 178 – 191.

Bowden P, Breemen O van, Hutchinson J, Turner DC (1971). Palaeozoic and Mesozoic Age Trends for some Ring Complexes in Niger and Nigeria. Nature, 259: 297 – 299.

Grapher5 (2004). Graphing System. Golden Software Inc. Golden, Colorado. www.goldensoftware.com.,

ILWIS 3.3 Academic (2005). ITC, RSG/GSD.

MacLeod WN, Turner DC, Wright EP (1965). The Geology of the Jos Plateau, 1: General Geology. Geological Survey of Nigeria. Bull., 32, 118 pp.

Maltman A (1990). Geological Maps – An Introduction. John Wiley & Sons Ltd, Baffins Lane, Chichester, West Sussex, England.

Olasehinde PI, Awojobi MO (2004). Geological and Geophysical Evidences of a North – South Fracture System East and West of the Upper Gurara River in Central Nigeria. Water Resources Journal, Nigerian Association of Hydrogeologist, 15: 33 –37.

Oluyide PO (1988). Structural Trends in the Nigerian Basement Complex. Precambrian Geology of Nigeria. Geological Survey of Nigeria Publication. 93 – 98.

Oyawoye MO (1964). The Geology of the Nigerian Basement Complex. Journal of Nigeria Mining. Geology and Metallurgical Society, 1(2): 87 – 103.

Oyawoye MO (1972). The Basement Complex of Nigeria, in Dessauwagie TFJ, Whiteman AJ (Eds). Africa Geology, University of Ibadan. 67 – 99

Rahaman MA, Breeman O van, Benner JN, Bowden P (1984). Age Migration of Anarogenic Ring Complexes in Northern Nigeria. Journal Geological. 92: 173 – 184.

Surfer9 (2009). Surface Mapping System. Thematic Mapping System. Golden Software Inc. Golden, Colorado. www.goldensoftware.com,.

Turner DC (1989). Structure and Petrology of the Younger Granite Ring Complexes, in Kogbe CA (Ed). Geology of Nigeria, Rock View International, France. 175 – 190.

Udoh AN (1988). An Interpretation of Satellite Imageries of Nigeria $7^0$40'N. Precambrian Geology of Nigeria. Geological Survey of Nigeria Publication. 99 – 102.

Wright JB (1976). Fracture System in Nigeria and Initiation of Fracture Zones in the South Atlantic. Tectonophysics. 34: 43 – 47.